Effective zero-thickness model for a conductive membrane driven by an electric field

Effective zero-thickness model for a conductive membrane driven by an electric field

Falko Ziebert,[1] Martin Z. Bazant,[2] and David Lacoste[1]
[1]*Laboratoire de Physico-Chimie Théorique, UMR CNRS Gulliver 7083, ESPCI, 10 rue Vauquelin, F-75231 Paris, France*
[2]*Department of Chemical Engineering and Department of Mathematics, Massachusetts Institute of Technology, Cambridge, Massachusetts 02139, USA*

(Received 2 November 2009; revised manuscript received 11 January 2010; published 11 March 2010)

The behavior of a conductive membrane in a static (dc) electric field is investigated theoretically. An effective zero-thickness model is constructed based on a Robin-type boundary condition for the electric potential at the membrane, originally developed for electrochemical systems. Within such a framework, corrections to the elastic moduli of the membrane are obtained, which arise from charge accumulation in the Debye layers due to capacitive effects and electric currents through the membrane and can lead to an undulation instability of the membrane. The fluid flow surrounding the membrane is also calculated, which clarifies issues regarding these flows sharing many similarities with flows produced by induced charge electro-osmosis (ICEO). Nonequilibrium steady states of the membrane and of the fluid can be effectively described by this method. It is both simpler, due to the zero thickness approximation which is widely used in the literature on fluid membranes, and more general than previous approaches. The predictions of this model are compared to recent experiments on supported membranes in an electric field.

DOI: 10.1103/PhysRevE.81.031912 PACS number(s): 87.16.−b, 82.39.Wj, 05.70.Np

I. INTRODUCTION

Bilayer membranes formed from phospholipid molecules are an essential component of the membranes of cells. The mechanical properties of equilibrium membranes are characterized by two elastic moduli, the surface tension and the curvature modulus [1], which typically depend on the electrostatic properties of the membranes [2]. Understanding how these properties are modified when the membrane is driven out of equilibrium is a problem of considerable importance to the physics of living cells. A membrane can be driven out of equilibrium in many ways, for instance by ion concentration gradients or electric fields, either applied externally or generated internally.

The external application of electric fields on lipid films is used to produce artificial vesicles (by electroformation), as well as to create holes in the membrane (by electroporation) [3]. Both processes are important for biotechnological applications, they are widely used experimentally although they are still rather poorly understood. The generation of ion concentration gradients by internal means is controlled in biological cells by membrane-bound ion pumps and channels, which play key roles in many areas of biology [4].

The nonequilibrium fluctuations of membranes including ion channels and pumps were first analyzed in Refs. [5,6] by means of an hydrodynamic theory. Artificially made active membranes inspired by these ideas were then studied experimentally [7–9]. Several theoretical studies followed, mainly motivated by the question of how to model nonequilibrium effects produced by protein conformation changes [10–13]. One limitation of existing active membrane models is that they do not describe electrostatic effects associated with ion transport in details. In previous papers by our group [14,15], we have addressed this limitation by studying a theoretical model for a membrane with a finite conductivity transverse to the membrane plane (due for instance to ion channels or pumps) using electrokinetic equations [16–18]. Our work complements Ref. [19], where the correction to the elastic moduli of a membrane in a dc electric field were calculated using an approach purely based on electrostatics (no currents). It is also inspired by Refs. [20,21]. where similar problems were considered using electrokinetic equations. In contrast to these studies, our approach focuses on the nonequilibrium case, where electrokinetic corrections to the elastic moduli arise due to currents through the membrane.

In particular, a negative correction to the surface tension arises due to capacitive effects, also called Lippman tension [22]. This negative tension leads to instabilities as can be understood from the high-salt limit [23]. A first experimental proof of the destabilizing effect of the electric field on a stack of lipid membranes was brought by x-ray scattering studies [24]. Recently, the lowering of the tension due to electrostatic or electrokinetic effects has been observed experimentally with supported membranes subjected to an ac electric field [25] and in active membranes [9].

The resulting flow fields around the undulating membrane are interpreted within the framework of "induced charge electro-osmosis" (ICEO) [18,26,27]. Similar flow patterns within vesicles subject to ac electric fields have been observed experimentally and analyzed theoretically in Ref. [28]. The deformation of lipid vesicles in alternating fields in various medium conditions has been modeled theoretically in Refs. [29,30]. All these studies show that lipid membranes in electric fields present a rich panel of possible behaviors [31,28].

This paper extends previous work [14,15], by providing an effective zero-thickness membrane model that contains both capacitive effects and ionic currents. In a first attempt [14], a zero-thickness membrane model has been proposed with the boundary condition (BC) of zero electric field at the membrane. Although the shape of the potential was acceptable, the charge distribution had the wrong sign and the elastic moduli were orders of magnitude too small. A model with finite membrane thickness and dielectric constant has thus been considered in Ref. [15], leading to correct signs of the

charge distribution and correct orders of magnitude of the elastic moduli. However, this model needed approximations and finally numerical evaluations. In view of this, we present here an improved zero-thickness model, by using the more realistic BC of a dielectric interface sustaining Faradaic currents [32]. Although this Robin-type BC has been introduced in Ref. [15], its consequences were not developed. In particular this model leads to simple analytical expressions for the corrections to the elastic constants of the membrane. The model clearly captures both nonequilibrium effects due to ion currents and equilibrium effects, of capacitive nature. We also calculate the flow field around the membrane, which has in fact the opposite sign as compared to the one of Ref. [15] for the zero-thickness case, and is thus similar to standard ICEO flow fields. The presented effective zero-thickness model for a dc-field driven conductive membrane is simple enough to be the starting point of more refined further studies.

The work is organized as follows: in Sec. II we describe the equations for the charges in the electrolyte. A special emphasis is put on the boundary conditions which is the crucial point here. Then the base state solution corresponding to a flat membrane is calculated in Sec. III. In Sec. IV we calculate the leading order contributions to the electric and ion density fields for a spatially modulated membrane height and analyze the corresponding hydrodynamic flows around the membrane. Using the boundary conditions for the stress tensor at the membrane (which includes Maxwell and hydrodynamic stresses), we calculate in Sec. V the growth rate of membrane fluctuations. In Sec. VI, our results are discussed and compared to previous calculations and to related experiments.

II. MODEL EQUATIONS

We consider a steady (dc) current driven by a voltage V between two electrodes at a fixed distance L, applied to an initially flat membrane located initially at $z=0$. The membrane is embedded in an electrolyte of monovalent ions with densities n^+ and n^-. The membrane has channels for both ion species but is itself neutral (no fixed charges at the membrane). The channels/pumps are assumed to be homogeneously distributed in the membrane and enter only in the effective conductance G, as introduced below. For the effect of nonuniform distributions of channels/pumps in membranes we refer to Refs. [11,33]. A point in the membrane is characterized by its Monge representation (valid in the limit of small undulations) by introducing a height function $h(\mathbf{r}_\perp)$, where $\mathbf{r}_\perp$ is a two-dimensional in-plane vector.

In the electrolyte, the governing equation for the electric potential ϕ is Poisson's equation

$$\nabla^2\phi = -\frac{1}{\epsilon}(en^+ - en^-). \tag{1}$$

Here e is the elementary charge and ϵ is the dielectric constant of the electrolyte. For the sake of simplicity, we assume a symmetric 1:1 electrolyte, so that far away from the membrane $n^+=n^-=n^*$. We also assume that the total system is electrically neutral.

The densities of the ion species are assumed to obey the Poisson-Nernst-Planck equations for a dilute solution

$$\partial_t n^\pm + \boldsymbol{\nabla}\cdot\mathbf{j}^\pm = 0, \tag{2}$$

with ionic current densities

$$\mathbf{j}^\pm = D\left(-\boldsymbol{\nabla}n^\pm \mp n^\pm\frac{e}{k_BT}\boldsymbol{\nabla}\phi\right), \tag{3}$$

where k_BT is the thermal energy. We have assumed that both ion types have the same diffusion coefficient D, and neglected various corrections for concentrated solutions [34]. We consider a steady-state situation and use the Debye-Hückel approximation by linearizing the concentrations $n^\pm = n^* + \delta n^\pm$, leading to

$$\nabla^2\phi = -\frac{e}{\epsilon}(\delta n^+ - \delta n^-), \tag{4}$$

$$\boldsymbol{\nabla}\cdot\left(-\boldsymbol{\nabla}\delta n^\pm \mp \frac{en^*}{k_BT}\boldsymbol{\nabla}\phi\right) = 0. \tag{5}$$

For symmetric binary electrolytes, it is useful to introduce *half* of the charge density [32,35],

$$\rho = e\frac{\delta n^+ - \delta n^-}{2}. \tag{6}$$

The sum of the two ionic concentrations, $\delta n^+ + \delta n^-$, turns out not to be a relevant variable since it is decoupled from the field at small applied voltages [35]. Moreover, since we have considered a steady state and a symmetric situation, there is no net particle current. We also define

$$\mathbf{j}^\rho = \frac{\mathbf{j}^+ - \mathbf{j}^-}{2} = -D\,\boldsymbol{\nabla}\left(\rho + \frac{e^2n^*}{k_BT}\phi\right), \tag{7}$$

which represents half of the electric current density, and we obtain the equations

$$\nabla^2\phi = -\frac{2}{\epsilon}\rho, \tag{8}$$

$$\nabla^2\rho + \frac{e^2n^*}{k_BT}\nabla^2\phi = 0. \tag{9}$$

Combining Eqs. (8) and (9) leads to $(\nabla^2-\kappa^2)\rho=0$, where

$$\kappa^2 = \frac{2e^2n^*}{\epsilon k_BT} \tag{10}$$

and $\kappa^{-1}=\lambda_D$ is the Debye length that defines the characteristic length scale for charge relaxation in the electrolyte.

Boundary conditions

At the electrodes located at $z=\pm\frac{L}{2}$, we externally impose the voltage leading to

$$\phi\left(z=\pm\frac{L}{2}\right) = \pm\frac{V}{2}. \tag{11}$$

This BC is oversimplified for real electrodes, since it neglects interfacial polarization across the double layers pass-

ing Faradaic currents [32,36], which makes the voltage imposed across the electrolyte, outside the double layers, different from the applied voltage. Since we focus on the membrane dynamics, however, electrode polarization is inconsequential, and the voltage V in the model simply serves as a means to apply a steady dc current, which could be directly measured or imposed in experiments testing our theory. We assume in the following that the distance between the electrodes is much larger then the Debye length, $L \gg \lambda_D = \kappa^{-1}$. In that case, the bulk electrolyte is quasineutral, $n^+ = n^- = n^*$, with negligible charge density (compared to the total salt concentration),

$$\rho\left(z = \pm \frac{L}{2}\right) = 0. \tag{12}$$

Since the conductivity of a quasineutral electrolyte is constant, the applied uniform current is equivalent to an applied electric field far from the membrane.

As we will see, the BC at the membrane is crucial to recover the correct physical behavior. Let $\mathbf{n}$ be the vector normal to the membrane. In the simple zero-thickness model proposed in Ref. [14] the Neumann BC,

$$(\mathbf{n} \cdot \boldsymbol{\nabla}) \phi_{|z=h} = 0, \tag{13}$$

was used for the potential, corresponding to a vanishing normal component of the electric field at the membrane. Thus, the dielectric mismatch between the electrolyte and the membrane was accounted for only approximatively. When compared to the full finite thickness calculation, the agreement was poor. To address this issue, a more general Robin-type BC was introduced [15]

$$\lambda_m (\mathbf{n} \cdot \boldsymbol{\nabla}) \phi_{|z=h^+} = \lambda_m (\mathbf{n} \cdot \boldsymbol{\nabla}) \phi_{|z=h^-} = \phi(h^+) - \phi(h^-), \tag{14}$$

where

$$\lambda_m = \frac{\epsilon}{\epsilon_m} d \tag{15}$$

is a length scale that contains the membrane thickness d and the ratio of the dielectric constant of the electrolyte, ϵ, and of the membrane, ϵ_m. This BC (with one side held at constant potential) was originally developed for electrodes sustaining Faradaic current [32,36–38] or charging capacitively [18,35]. In that context the analog of our membrane is a Stern monolayer of solvent molecules or a thin dielectric coating, such as a native oxide, on a metallic surface, and λ_m is denoted λ_S. Note that this BC has also been used in Ref. [21].

The modified boundary condition (14) introduces a new dimensionless parameter [32],

$$\delta_m = \kappa \lambda_m = \frac{\lambda_m}{\lambda_D} = \frac{\epsilon \kappa}{\epsilon_m / d} = \frac{C_D}{C_m}. \tag{16}$$

For a blocking or "ideally polarizable" surface, which does not pass normal current and only allows capacitive charging of the double layer, this parameter controls the relative importance of the capacitance of the surface (here, the membrane) $C_m = \epsilon_m / d$ compared to that of the diffuse part of the double layer, $C_D = \epsilon \kappa$. The BC [Eq. (14)] then implies that these capacitances are effectively coupled in series in an equivalent-circuit representation of the double layer + membrane surface [35]. For a surface sustaining normal current, either by electron-transfer reactions at an electrode or by ionic flux through a membrane, the situation is more complicated. It can be shown that the same electrostatic BC [Eq. (14)] remains valid for a thin dielectric layer, as long as it has zero total free charge [34], which is typical for membranes containing a high density of fixed counter charge. However, the same parameter δ_m no longer plays the role of a capacitance ratio. Instead, it controls the effect of diffuse charge on the normal current, the so-called "Frumkin correction" to reaction kinetics in electrochemistry, reviewed in Ref. [36]. Two distinct regimes were first identified in Ref. [32] in the context of electrolytic cells and recently extended to galvanic cells [36]: (i) the "Helmholtz limit" $\delta_m \gg 1$, where most of the double layer voltage is dropped across the surface or membrane and the diffuse-layer has no effect on the current, and (ii) the "Gouy-Chapman limit" $\delta_m \ll 1$ where the diffuse layer carries all of the voltage and thus determines the current. In the Helmholtz limit, the Robin BC [Eq. (14)] reduces to the Neumann BC [Eq. (13)] used in Ref. [15], so that paper analyzed the limit where the diffuse charge is small and has little effect on the current. In this paper we consider the general case of finite δ_m.

III. BASE STATE

The base state of the problem is a flat membrane. The electric field, assumed to be perfectly aligned in z direction, is then perpendicular to the membrane. In the bulk fluid, the system is completely characterized by the electrostatic potential $\phi_0(z)$ [or by the field $E_0(z) = E_0^z(z) = -\partial_z \phi_0$], by the steady-state ion distribution $\rho_0(z)$, as well as by the pressure $P_0(z)$. Inside the membrane, an internal electrostatic potential $\phi_0^m(z)$ (and field E_0^m) is present.

Equations (8) and (9) are readily solved leading to the charge distribution

$$\rho_0(z) = \begin{cases} \rho_m e^{-\kappa z}; & z > 0 \\ -\rho_m e^{\kappa z}; & z < 0 \end{cases}, \tag{17}$$

and to the potential

$$\phi_0(z) = \begin{cases} \dfrac{2}{\epsilon \kappa^2}\left[\dfrac{j_m}{D}\left(z - \dfrac{L}{2}\right) - \rho_m e^{-\kappa z}\right] + \dfrac{V}{2}; & z > 0 \\ \dfrac{2}{\epsilon \kappa^2}\left[\dfrac{j_m}{D}\left(z + \dfrac{L}{2}\right) + \rho_m e^{\kappa z}\right] - \dfrac{V}{2}; & z < 0 \end{cases}. \tag{18}$$

Here $j_m = -j^\rho$ is the electric current density and

$$\rho_m = \frac{\rho(z = 0^+) - \rho(z = 0^-)}{2} =: \frac{1}{2}[\rho_0]_{z=0} \tag{19}$$

represents the jump in the charge density across the membrane. We have introduced the notation

$$[f]_{z=a} = f(z = a^+) - f(z = a^-), \tag{20}$$

by which we denote the jump of the field f at position $z = a$. Note that the jump in the charge density ρ_m at the membrane

can be interpreted in terms of a surface dipole localized on the membrane. The existence of this surface dipole is the physical reason for the discontinuity of the potential at the membrane.

At the membrane, the Robin-type BC reads

$$\lambda_m \partial_z \phi_{|z=0+} = \lambda_m \partial_z \phi_{|z=0-} = [\phi]_{z=0}. \tag{21}$$

Although the membrane has a zero thickness in this model, one can still define an internal field E_0^m and an internal potential $\phi_0^m(z)$. This is done by keeping a finite thickness d at first, and then take the limit $d \to 0$, see Ref. [15] for details. Continuity of the potential at the membrane boundaries then implies a constant internal field $E_0^m = -[\phi_0]_{z=0}/d$ and the internal potential $\phi_0^m(z) = [\phi_0]_{z=0} z/d$. Using Eq. (18), we obtain

$$E_0^m = -\frac{1}{d}\left[\frac{2}{\epsilon\kappa^2}\left(-\frac{j_m L}{D} - 2\rho_m\right) + V\right]. \tag{22}$$

Now one has to determine ρ_m and j_m. Using Eq. (21), one obtains the jump in the charge density

$$\rho_m = \frac{\frac{\epsilon\kappa^2}{2}V - \frac{j_m}{D}(L + \lambda_m)}{2 + \kappa\lambda_m}. \tag{23}$$

Two remarks on this derivation are in order: first, Eq. (23) illustrates that the asymmetry of the charge distribution results either from the accumulation of charges due to the applied voltage (a capacitive effect proportional to V, present also for nonconductive membranes) or due to ionic currents across the membrane (a nonequilibrium effect proportional to j_m present only for conductive membranes). Second, the expressions for $\rho(z)$, $\phi(z)$, ρ_m derived above are independent of the response of the ion channels and thus remain *unchanged* if a nonlinear ion channel response is used. Only the expression for the current j_m, that enters as a parameter, will be affected by such a nonlinearity. For precisely that reason, the general form of the base state does not depend on the mechanism that has created the asymmetry of charge distribution or the ionic currents (external due to an applied field or internal due to pumps).

To determine the current density j_m at the membrane position, we use a linear response approach (for nonlinear ionic response, see for instance Refs. [4,21,39])

$$j^\rho_{|z=0} = -\frac{G}{e}[\mu^\rho]_{z=0}, \tag{24}$$

where μ^ρ is the chemical potential per particle and G is the membrane conductance per unit surface (across the membrane, not in plane). We assumed equal G for both ion species. In the bulk one has $j^\rho = -\frac{eDn^*}{k_B T}\partial_z \mu^\rho$, which leads to the usual expression for the (electro-)chemical potential, $\mu^\rho = k_B T \frac{\rho}{en^*} + e\phi$. By equating

$$-j_m = j^\rho_{|z=0} = -\frac{G}{e}\left(\frac{k_B T}{en^*}[\rho_0]_{z=0} + e[\phi_0]_{z=0}\right), \tag{25}$$

we finally arrive at the simple expression

$$j_m = -j^\rho = \frac{GV}{1 + \frac{2}{\epsilon\kappa^2 D}GL}. \tag{26}$$

This relation is consistent with the usual electric circuit representation of ion channels in a membrane that is surrounded by an electrolyte [4,14]. As far as the sign convention of the currents is concerned, the cathode (toward where the cations drift) is located at $z=-L/2$ and the anode at $z=L/2$. Thus j_m is positive, in accordance with the usual convention for transport of positive charges from the anode to the cathode. Insertion of j_m into ρ_m yields

$$\rho_m = \frac{\epsilon\kappa^2}{2}V\frac{1 - \frac{2}{\epsilon\kappa^2 D}G\lambda_m}{\left(1 + \frac{2}{\epsilon\kappa^2 D}GL\right)(2 + \kappa\lambda_m)}. \tag{27}$$

Note that this derivation is general and holds for any value of $\delta_m = \kappa\lambda_m$. The jump in the charge distribution at the membrane is positive (equivalent to a surface dipole oriented in the +z direction), $\rho_m > 0$, for poorly conductive membranes when $\lambda_m < \epsilon\kappa^2 D/(2G)$. This corresponds well to the case of biological membranes (see Sec. VI), which are typically much less conductive than the surrounding electrolyte. In this case, positive charges pile up at the side of the positive electrode (and due to symmetry, negative charges will do the same on the other side), leading to $\rho_m > 0$. For highly conductive membranes, this piling up effect does not arise anymore, because positive charges are able to cross the membrane easily. This results in a negative jump of the charge distribution at the membrane (equivalent to a surface dipole oriented in the $-z$ direction) when $\lambda_m > \epsilon\kappa^2 D/(2G)$. The threshold on membrane conductance (per unit area) is given by the conductance of a layer of electrolyte of thickness equal to the membrane thickness times the ratio of dielectric constants, i.e., $G_c = \epsilon_m e^2 n^* D/\epsilon k_B T d$. This threshold G_c is much too high to be accessible with biological membranes (even in the best conditions of low salt). However, with artificial membranes of very high conductivity, this effect may be observable. We now understand why the zero thickness model with the simple BC, Eq. (13), is not realistic for biological membranes. Indeed, it corresponds to $\lambda_m = \infty$, implying $\rho_m < 0$. We note that by performing the limit $\lambda_m \to \infty$ in Eq. (27), one regains the results for the zero-thickness model of Ref. [15] with BC Eq. (13).

To complete the description of the base state, we have to consider the total stress tensor

$$\tau_{ij} = -P\delta_{ij} + \eta(\partial_i v_j + \partial_j v_i) + \epsilon\left(E_i E_j - \frac{1}{2}\delta_{ij}E^2\right) \tag{28}$$

at the membrane. It contains the pressure, the viscous stresses in the fluid and the Maxwell stress due to the electrostatic field. We denote by η the viscosity of the electrolyte and by $\mathbf{v}$ its velocity field. The electric field is given by $\mathbf{E} = -\nabla\phi$.

In the base state, where the membrane is flat and the electric field is oriented in z direction, from $\nabla\cdot\tau=0$ we get $\partial_z P_0=\frac{\epsilon}{2}\partial_z[(\partial_z\phi_0)^2]=-2\rho_0\partial_z\phi_0$. By using Eqs. (17) and (18) and imposing $P(z\to\infty)=0$, this is readily solved leading to

$$P_0(z>0)=\frac{4}{\epsilon\kappa^3}\left(\frac{\rho_m j_m}{D}e^{-\kappa z}+\frac{\kappa\rho_m^2}{2}e^{-2\kappa z}\right), \tag{29}$$

and similarly with $z\to -z$ for $z<0$. For the stress we thus get

$$\tau_{zz,0}(z>0)=\tau_{zz,0}(z<0)=\frac{2}{\epsilon\kappa^4 D^2}j_m^2. \tag{30}$$

Note that the stress is constant and is due to the current density j_m, with no contributions from the induced charges ρ_m. At the membrane, the stress is balanced. In addition to the part of the stress tensor due to the electric field in the electrolyte, there also is the part due to the electric field inside the membrane, already mentioned above. For the force balance in the base state however, this contribution vanishes is thus not important.

IV. LEADING ORDER CONTRIBUTION OF MEMBRANE FLUCTUATIONS

In the following, we derive the corrections to the base state to first order in the membrane height $h(\mathbf{r}_\perp)$. From such a calculation, we obtain the growth rate of membrane fluctuations by imposing the BC for the normal stress at the membrane. From this growth rate, we then can identify electrostatic and electrokinetic corrections to the elastic moduli of the membrane.

A. Electrostatic problem

We use here the quasistatic approach [15,19] by assuming that membrane fluctuations are much slower than the characteristic diffusion time $\tau_D=\frac{1}{D\kappa^2}$ of the ions to diffuse on a Debye length. With the definition of the Fourier transform $f(\mathbf{k}_\perp,z)=\int d\mathbf{r}_\perp e^{-i\mathbf{k}_\perp\cdot\mathbf{r}_\perp}f(\mathbf{r}_\perp,z)$, we expand the electric field and the charge density as

$$\phi(\mathbf{k}_\perp,z)=\phi_0(z)+\phi_1(\mathbf{k}_\perp,z), \tag{31}$$

$$\rho(\mathbf{k}_\perp,z)=\rho_0(z)+\rho_1(\mathbf{k}_\perp,z), \tag{32}$$

where $\mathbf{k}_\perp$ lies in the plane defined by the membrane and $\phi_0(z)$, $\rho_0(z)$ are the base state solutions given by Eqs. (17) and (18).

Let us introduce l, the inverse characteristic length scale of the electrostatic potential near the slightly undulated membrane, defined by

$$l^2=k_\perp^2+\kappa^2. \tag{33}$$

As shown in Appendix A, first-order corrections to the potential and charge density read

$$\phi_1(\mathbf{k}_\perp,z)=-\frac{2}{\epsilon}\rho_m\frac{h(\mathbf{k}_\perp)}{l}e^{-lz},$$

$$\rho_1(\mathbf{k}_\perp,z)=\kappa^2\rho_m\frac{h(\mathbf{k}_\perp)}{l}e^{-lz}, \tag{34}$$

for $z>0$ and a symmetric expression (i.e., with e^{lz}) for $z<0$.

B. Linear hydrodynamic flow

When the membrane starts to undulate with small amplitude $h(\mathbf{r}_\perp)$, a flow is induced in the surrounding electrolyte. Using again the quasistatic assumption and low Reynolds number, this flow is governed by incompressibility and the Stokes equation,

$$\nabla\cdot\mathbf{v}=0,$$

$$-\nabla p+\eta\nabla^2\mathbf{v}+\mathbf{f}=0, \tag{35}$$

where $\mathbf{f}$ is a body force density due to the electric field. Introducing the triad [1,40] of unit vectors $(\hat{\mathbf{k}}_\perp,\hat{\mathbf{n}},\hat{\mathbf{t}})$ with $\hat{\mathbf{k}}_\perp=\mathbf{k}_\perp/k_\perp$, $\hat{\mathbf{n}}=\hat{z}$ and $\hat{\mathbf{t}}=\hat{\mathbf{k}}_\perp\times\hat{\mathbf{n}}$, we get

$$\partial_z v_z+i\mathbf{k}_\perp\cdot\mathbf{v}_\perp=0, \tag{36}$$

$$-i\mathbf{k}_\perp p+\eta(\partial_z^2-k_\perp^2)\mathbf{v}_\perp+\mathbf{f}_\perp=0, \tag{37}$$

$$-\partial_z p+\eta(\partial_z^2-k_\perp^2)v_z+f_z=0, \tag{38}$$

$$\eta(\partial_z^2-k_\perp^2)v_t+f_t=0. \tag{39}$$

Two forces drive the flow: one is given by the coupling to the membrane, enters via the BC, and is discussed below. The second one is the bulk force due to the electric field acting on the charge distribution and reads $\mathbf{f}=Q\mathbf{E}=-2\rho\nabla\phi$. Note that one has to use the total charge density, $Q=2\rho$. To leading order in the membrane height, this driving force is $\mathbf{f}=-2\rho_0\nabla\phi_1-2\rho_1\nabla\phi_0+O(h^2)$ with components

$$\mathbf{f}_\perp=-2\rho_0(z)i\mathbf{k}_\perp\phi_1(\mathbf{k}_\perp,z),$$

$$f_z=-2\rho_0(z)\partial_z\phi_1(\mathbf{k}_\perp,z)-2\rho_1(\mathbf{k}_\perp,z)\partial_z\phi_0(z), \tag{40}$$

and $f_t=0$. Because of the latter, Eq. (39) is decoupled and trivial.

To solve for v_z, $\mathbf{v}_\perp$, and p we proceed as follows: using incompressibility for the perpendicular fluid velocity, one solves for the pressure. Insertion into Eq. (38) then yields a single equation for v_z, for $z>0$

$$(\partial_z^2-k_\perp^2)^2 v_z=\frac{2}{\eta}k_\perp^2\phi_1\partial_z\left(\rho_0+\frac{\epsilon}{2}\kappa^2\phi_0\right). \tag{41}$$

As the driving term on the r.h.s. is a constant times e^{-lz} (due to ϕ_1), by imposing $v_z(z\to\pm\infty)=0$ the solution is of the form

$$v_z=(B+Cz)e^{-k_\perp z}+Fe^{-lz}. \tag{42}$$

The coefficient F is determined by the driving force $\mathbf{f}$, but two more BCs are needed. At the membrane, continuity of the normal velocity imposes $v_z(0^+)=v_z(0^-)=\partial_t h(\mathbf{r}_\perp)=sh(\mathbf{k}_\perp)$ where we have introduced the growth rate for mem-

brane fluctuations, s, from the temporal Fourier representation $h(t) \propto e^{st}$. Note that s is also a function of $\mathbf{k}_\perp$. The continuity of the tangential velocity, $\mathbf{v}_\perp(0^+)=\mathbf{v}_\perp(0^-)=0$, together with the incompressibility implies a second BC for v_z, namely $\partial_z v_{z|0^+}=\partial_z v_{z|0^-}=0$. With the notation

$$\alpha = \frac{4\rho_m j_m}{\epsilon D \eta \kappa^4}, \tag{43}$$

which quantifies the amplitude of the ICEO flow, see below, the velocity and pressure fields in the domain $z>0$ read

$$v_z(z>0) = h(\mathbf{k}_\perp)\left[s(1+k_\perp z)e^{-k_\perp z} - \alpha k_\perp \left(k_\perp z - \frac{k_\perp}{l} - \frac{k_\perp^2 z}{l} \right) e^{-k_\perp z} - \alpha \frac{k_\perp^2}{l} e^{-lz} \right], \tag{44}$$

$$\mathbf{v}_\perp(z>0) = h(\mathbf{k}_\perp) i\mathbf{k}_\perp \left[-sze^{-k_\perp z} - \alpha \left(1 - k_\perp z + \frac{k_\perp^2 z}{l} \right) e^{-k_\perp z} + \alpha e^{-lz} \right], \tag{45}$$

$$p(z>0) = h(\mathbf{k}_\perp)\eta \left\{ 2k_\perp \left[s - \alpha \left(k_\perp - \frac{k_\perp^2}{l} \right) \right] e^{-k_\perp z} + \alpha e^{-lz} + \frac{4\rho_m^2}{\epsilon \eta l} e^{-(l+\kappa)z} \right\}. \tag{46}$$

The solutions for $z<0$ can be obtained by symmetry operations: $v_z(z<0)$ is obtained by performing the mirror operation with respect to the plane defined by the membrane, $z \to -z$, in the formula for $v_z(z>0)$. Similarly $-\mathbf{v}_\perp(z<0)$ and $-p(z<0)$ are obtained by doing this operation on $\mathbf{v}_\perp(z>0)$ and $p(z>0)$, respectively.

In the absence of electric effects, $\rho_m=0=j_m$, one gets the typical flow induced by a membrane bending mode [41,42]. An additional flow field due to the membrane currents arises that has the form of an ICEO flow [18]. A detailed discussion of this effect is postponed to Sec. VI, but we stress that the additional flow is purely due to membrane conductivity (since $\alpha \propto j_m \propto G$), and is a nonequilibrium effect. For nonconductive membranes this flow vanishes but there still is charge accumulation ($\rho_m \neq 0$) in the Debye layers, leading via the pressure field, Eq. (46), to corrections to surface tension and bending rigidity proportional to ρ_m^2.

V. GROWTH RATE OF MEMBRANE FLUCTUATIONS

To discuss the dynamics of the membrane, we still have to determine the growth rate s of the membrane. The elastic properties of the membrane are described by the standard Helfrich free energy

$$F_H = \frac{1}{2}\int d^2\mathbf{r}_\perp [\Sigma_0 (\nabla h)^2 + K_0 (\nabla^2 h)^2], \tag{47}$$

where Σ_0 is the bare surface tension and K_0 the bare bending modulus of the membrane. Force balance on the membrane implies that the restoring force due to the membrane elasticity is equal to the discontinuity of the normal-normal component of the stress tensor defined in Eq. (28)

$$-[\tau_{zz,1}]_{z=0} = -\frac{\partial F_H}{\partial h(\mathbf{r}_\perp)} = (-\Sigma_0 k_\perp^2 - K_0 k_\perp^4) h(\mathbf{k}_\perp). \tag{48}$$

We should stress that the coupled electrostatics-hydrodynamics problem under investigation can *not* be formulated only in terms of bulk forces, i.e., $\mathbf{f}$ and the divergence of a stress tensor, because the hydrodynamic and Maxwell stress tensors enter the BC Eq. (48) explicitly. For this reason, the force localized on the membrane surface is *a priori* unknown, i.e., must be determined by BCs for the velocity and the stress.

Equation (48) determines the growth rate $s=s(k_\perp)$ entering the normal stress difference. Details of the evaluation of $[\tau_{zz,1}]_{z=0}$ can be found in Appendix B. After isolating s and expanding in wave number $\mathbf{k}_\perp$, the growth rate $s(k_\perp)$ finally has the form

$$\eta k_\perp s(k_\perp) = -\frac{1}{4}(\Sigma_0 + \Delta\Sigma)k_\perp^2 - \Gamma_\kappa k_\perp^3 - \frac{1}{4}(K_0 + \Delta K)k_\perp^4. \tag{49}$$

The electrostatic corrections to the surface tension, $\Delta\Sigma = \Delta\Sigma_\kappa + \Delta\Sigma_m$, and to the bending modulus, $\Delta K = \Delta K_\kappa + \Delta K_m$ have been decomposed into outside contributions (due to the Debye layer, index κ) and inside contributions (due to the voltage drop at the membrane, index m). They are given by

$$\Delta\Sigma_\kappa = -4\frac{\rho_m^2}{\epsilon\kappa^3} - 16\frac{\rho_m j_m}{\epsilon\kappa^4 D}, \tag{50}$$

$$\Delta K_\kappa = \frac{3\rho_m^2}{\epsilon\kappa^5} \tag{51}$$

for the contributions due to the Debye layers and by

$$\Delta\Sigma_m = -\epsilon_m (E_0^m)^2 d, \tag{52}$$

$$\Delta K_m = \epsilon_m (E_0^m)^2 \left(\frac{d^3}{12} - \frac{\rho_m}{E_0^m}\frac{d}{\epsilon\kappa^3} \right), \tag{53}$$

for the contributions due to the field inside the membrane, cf. Eq. (22). In Eq. (49), we also obtain a purely nonequilibrium correction

$$\Gamma_\kappa = \frac{4\rho_m j_m}{\epsilon\kappa^5 D} = \frac{\eta}{\kappa}\alpha. \tag{54}$$

It corresponds to a term proportional to $k_\perp^3$ in the effective free energy of the membrane, which is forbidden for an equilibrium membrane but allowed in nonequilibrium. This particular contribution arises due to the electro-osmotic flows around the membrane (cf. Sec. VI C), as can be shown from a simple calculation using the Helmholtz-Smoluchowski equation for the electro-osmotic slip velocity near the membrane [15].

We should mention that an independent check of Eqs. (50) and (52) is provided by a direct integration of the lateral

pressure profile as shown in Appendix C. This route avoids the consideration of hydrodynamics but is limited to the calculation of the surface tension correction.

VI. DISCUSSION

Let us discuss the corrections to the membrane moduli, Eqs. (50)–(53) and compare them to previous theoretical work on this question. Two particular limits have been considered before: first, the high-salt limit ($\kappa \to \infty$) of a conductive membrane. In this case, one finds that the correction to the surface tension is only due to the inside field, since $\Delta\Sigma_\kappa \to 0$ and $\Delta\Sigma_m \to -\epsilon_m \frac{V^2}{d}$, in agreement with Ref. [23]. The corrections to the bending modulus were not considered in that reference, but can be obtained from the present calculation as $\Delta K_\kappa \to 0$ and $\Delta K_m \to \epsilon_m \frac{V^2}{12} d$, similar to the nonconductive case. In this limit, we get a simple expression for the ratio $\Delta K_m / \Delta\Sigma_m = -d^2/12$, which is thus independent of the applied voltage and proportional to the square of the membrane thickness. While this simple dependence on the thickness is restricted to the high-salt limit (where d is the only relevant length scale), the independence of voltage is *general*: the ratio $\Delta K / \Delta\Sigma$ is always independent of the applied voltage, since ρ_m, j_m, and E_0^m are proportional to V. This is a consequence of our use of a linear ohmic response for the membrane, linear electrostatics (Debye-Hückel approximation) for the electrolyte and of the assumption that the membrane does not carry any fixed charges. A dependence of the ratio on applied voltage, if it could be observed experimentally, would imply the violation of one of these assumptions.

The second situation considered in the literature is the case of a nonconductive membrane ($j_m = 0$, $\rho_m \neq 0$) with an arbitrary amount of salt [19]. For $G = j_m = 0$, the sum of the two corrections to the surface tension given by Eqs. (50) and (52) can be expressed as

$$\Delta\Sigma = -\frac{\epsilon_m V^2}{d} \frac{1 + \frac{\epsilon_m}{\epsilon\kappa d}}{\left(1 + \frac{\epsilon_m}{\epsilon\kappa^2 d/2}\right)^2}, \tag{55}$$

which agrees with the result of [19] (note that there, the membrane thickness was defined as $2d$). For the total bending modulus correction, we obtain

$$\Delta K = \frac{\epsilon_m d V^2}{12} \frac{\left(1 + \frac{3}{2}\frac{\epsilon_m}{\epsilon(\kappa d/2)^2} + \frac{9}{8}\frac{\epsilon_m}{\epsilon(\kappa d/2)^3}\right)}{\left(1 + \frac{\epsilon_m}{\epsilon\kappa d/2}\right)^2}. \tag{56}$$

This formula is of the same form as the one given in [19], but the numerical prefactors of the finite salt correction terms (second and third term in the upper bracket) differ slightly. This is most probably due to a difference in the boundary conditions which leads to differences in the expression of the potential inside the membrane, given by Eqs. (B9) and (B10). Nevertheless, the high-salt limit is correct and the overall shape of $\Delta K(\kappa)$ is well captured, as shown in the next section. Thus, our general results, Eqs. (50)–(53), extend the work of Ambjörnsson *et al.* to the case of a conductive membrane.

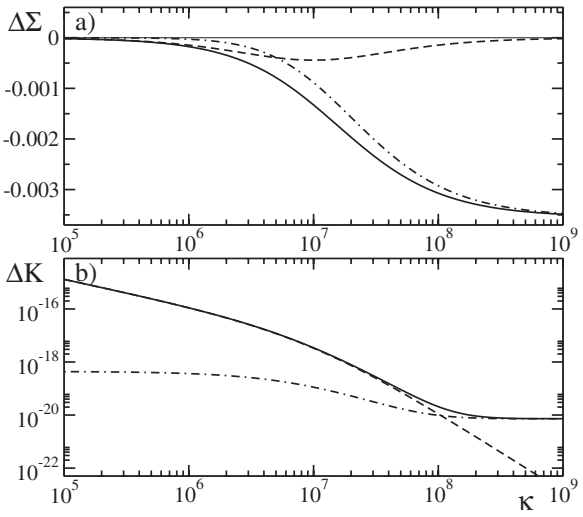

FIG. 1. Panel (a) shows the electrostatic corrections to the surface tension (in units of $\mathbf{N}\cdot\mathrm{m}^{-1}$) and panel (b) those to the bending modulus (units J) as a function of κ (units m^{-1}) in the nonconductive case, $G=0$. Dashed lines: contributions due to the Debye layer ($\Delta\Sigma_\kappa$ and ΔK_κ respectively). Dash-dotted lines: contributions due to the field inside the membrane ($\Delta\Sigma_m$ and ΔK_m respectively). Solid lines: sum of both corrections. The figure was made with the parameters given in the text and $V=1$ V, $L=1$ mm.

A. Effect of salt and membrane conductivity

With the expressions for the jump of the charge density at the membrane, Eq. (27), for the current density, Eq. (26), and for the internal field, Eq. (22), we can discuss the corrections to the membrane elastic constants given by Eqs. (50)–(53) in detail. In particular we obtain the dependence of these elastic moduli on the ionic strength of the electrolyte, and on the ion conductance of the membrane per unit area, G.

We have used the following parameters: dielectric constants are $\epsilon = 80\epsilon_0$ for the electrolyte and $\epsilon_m = 2\epsilon_0$ for the membrane. The membrane thickness is typically $d=5$ nm leading to $\lambda_m = \frac{\epsilon}{\epsilon_m} d = 200$ nm. The diffusion coefficient of ions is of the order of $D = 10^{-9}$ $\mathrm{m}^2\,\mathrm{s}^{-1}$, and the viscosity $\eta = 10^{-3}$ Pa s.

Figure 1(a) displays separately the contributions to the surface tension as a function of the inverse Debye length κ. The dashed line represents the contribution from the Debye layers, the dash-dotted line represents the contribution from the field inside the membrane and the solid line is the sum of both contributions. The value of the inverse Debye length κ, varies from $\kappa \simeq 10^6$ m^{-1} ($\lambda_D = 1$ μm) for pure water to $\kappa = 3.3 \times 10^9$ m^{-1} ($\lambda_D \simeq 0.3$ nm) for 1M NaCl [2]. Figure 1(b) shows the respective contributions to the membrane bending modulus. In this figure we have assumed that the membrane is nonconductive ($G=0$). As shown in Fig. 1, the contributions from the Debye layers dominate for low salt ($\kappa < 5 \times 10^6$ m^{-1} for $\Delta\Sigma$ and $\kappa < 10^8$ m^{-1} for ΔK). For high salt, the contributions from the membrane dominate, and approach the limiting values discussed above. In this case of

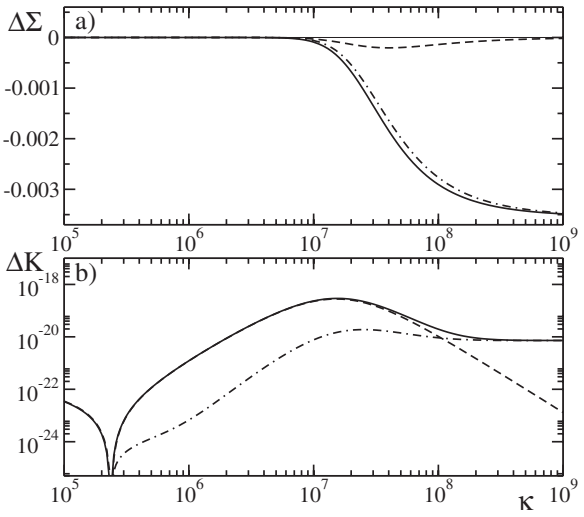

FIG. 2. Electrostatic corrections to the surface tension (panel a) and to the bending modulus (panel b) as a function of κ in a slightly conductive case ($G=0.1$ S m^{-2}). Dashed lines: contributions due to the Debye layer. Dash-dotted lines: contributions due to the field inside the membrane. Solid line: sum of both corrections. Parameters as in previous figure except for G.

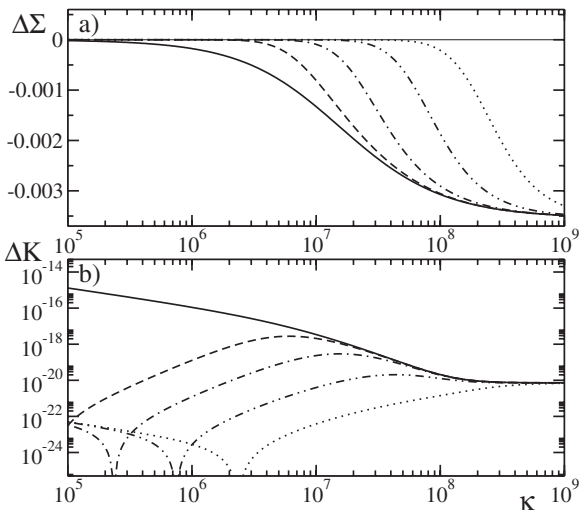

FIG. 3. Electrostatic corrections to the surface tension (panel a) and to the bending modulus (panel b) as a function of κ for different membrane conductivities. Parameters are as in the two previous figures except for G: solid line $G=0$; dashed line $G=0.01$; dash-dotted line $G=0.1$; dash-two-dots line $G=1$; dotted line $G=10$ in units of S m^{-2}.

zero conductivity, both the Debye and the inside contribution to the surface tension are always negative, and there is good agreement with previous treatments for nonconductive membranes [15,19].

Figure 2 displays the corrections to the elastic coefficients in the case where a finite membrane current j_m is present, induced by a small conductance per unit area $G=0.1$ S m^{-2}, for otherwise unchanged parameters. We find that this rather small conductance has already a large effect on both moduli: first, the effect of the Debye layers on the surface tension is suppressed and the contribution from the membrane is dominating. Second, the overall contribution gets relevant for higher salt than in the nonconductive case. The effect on the bending modulus is even more significant: although the Debye contribution is still dominating for about $\kappa < 10^8$ m^{-1}, it is much smaller in amplitude than in the nonconductive case (around 10^{-20} J compared to 10^{-17} J at $\kappa \simeq 5\times 10^6$ m^{-1}) and furthermore becomes nonmonotonous [15].

The effect of membrane conductance is highlighted in Fig. 3, where the total contributions to surface tension (panel a) and bending modulus (panel b) are shown as a function of the inverse Debye length κ for conductances per unit area in the range $G=0.01-10$ S m^{-2}, and otherwise unchanged parameters. We find that, except for the high-salt limit, the bending modulus correction tends to be reduced by increasing membrane conductance. To give some numbers, for a nonconductive membrane ($G=0$) and $V=1$ V, the jump in the charge density for $\kappa=2\times 10^7$ m^{-1} is $\rho_m=1.5\times 10^{23}$ $\frac{e}{\mathrm{m}^3}$. Already a small value of the conductance per unit area $G=0.1$ S m^{-2} halves the charge density to $\rho_m=8.6\times 10^{22}$ $\frac{e}{\mathrm{m}^3}$ and creates the current density $j_m=3.7\times 10^{17}$ $\frac{e}{\mathrm{m}^2\mathrm{s}}$, or 60×10^{-3} $\frac{\mathrm{A}}{\mathrm{m}^2}$. Conductances of biological membranes can be as high as $G=10$ S m^{-2}, which is the value for a squid axon, corresponding to a density of potassium channels of 0.5 μm^{-2} [4].

We also note that the distance between the electrodes L, i.e., the confinement, is a relevant parameter and influences the shape of Figs. 1 and 2. Here we have used a macroscopic distance ($L=1$ mm), corresponding to the experiments mentioned below. If L was instead of the order of microns, the suppression of the bending modulus correction due to membrane conductivity would be much less pronounced and the corresponding figure would become similar to the one given in Ref. [15]. Moreover, for high enough membrane conductivity, the Debye layer contribution to the surface tension can become positive, i.e., stabilizing. In fact, the sign of $\Delta\Sigma_\kappa$ is governed by a factor $-\frac{\epsilon D\kappa^2-2G\lambda_m}{(\epsilon D\kappa^2+2GL)^2}$. In a way similar as discussed in Sec. III concerning the sign of ρ_m, for $G>\frac{\epsilon D\kappa^2}{2\lambda_m}$ there is a sign change, rendering the correction positive for small κ. However, the denominator containing the distance L between the electrodes suppresses this effect for macroscopic distances. It can be seen only if L is small, e.g., $L=1$ μm as used in Ref. [15]. We note that the micron scale is particularly relevant to experiments with cell membranes submitted to electric fields [22]. It is also relevant to experiments that one could propose to test these ideas using microfluidics devices.

B. Membrane instability

Since the corrections to the membrane surface tension are typically negative (with the exception mentioned above), they can overcome the bare surface tension Σ_0. At this point, an instability toward membrane undulations sets in [23]. Our theory is able to go beyond previous modeling of this instability (still for early stages of the instability), which were limited to the high-salt limit and did not include electrostatic corrections to the bending modulus or hydrodynamic effects associated with the modulus Γ. The linear growth rate of the

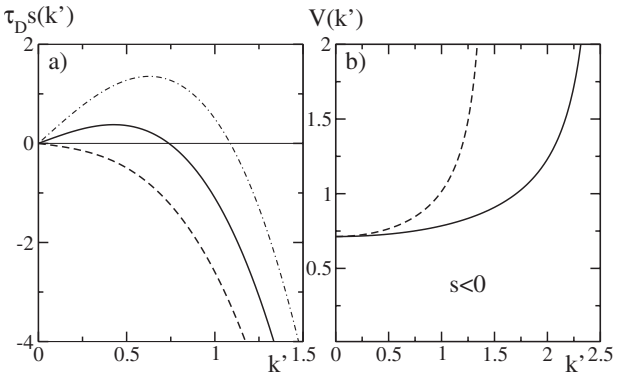

FIG. 4. (a) The renormalized growth rate or dispersion relation, $\tau_D s$, as a function of the rescaled wave number $k'=k_\perp/\kappa$ for three voltages: $V=0.7$ V (dashed line), $V=0.75$ V (solid line), $V=0.8$ V (dash-dotted line). (b) The neutral curve (solid line) separating the regions of $s>0$ and $s<0$, and the fastest growing wave number k_{fg} (dashed line) in the plane voltage vs rescaled wave number $k'=k_\perp/\kappa$. Parameters as previously except: no conductivity, $G=0$; $\kappa=2\cdot 10^7$ m^{-1}; $\Sigma_0=1$ mN m^{-1}; $K_0=10k_BT$.

membrane fluctuations is given by Eq. (49) and has the form

$$\eta s(k) = -\frac{1}{4}\tilde{\Sigma}k - \Gamma_\kappa k^2 - \frac{1}{4}\tilde{K}k^3, \tag{57}$$

where we have written simply k for $k_\perp$ and introduced the effective surface tension and modulus, $\tilde{\Sigma}=\Sigma_0+\Delta\Sigma$, $\tilde{K}=K_0+\Delta K$. Figure 4(a) shows this growth rate, or dispersion relation, in rescaled units where we scaled the wave vector by κ, $k'=k/\kappa$, and the time by the typical time for ions to diffuse a Debye length, $\tau_D=\frac{1}{D\kappa^2}$. The parameters are the same as in the previous sections for a nonconductive membrane, i.e., $G=0$. The control parameter is the external voltage V. Figure 4(a) shows the growth rate for three different levels of the voltage: the dashed line is for $V=0.7$ V, which lies below the threshold of the instability, all wave numbers are damped and the membrane is stable. The solid and the dash-dotted line correspond to $V=0.75$ V and $V=0.8$ V and are above threshold. A certain window of wave numbers $k \in]0,\ k_{\max}(V)[$ has positive growth rates and the membrane is thus unstable. This window gets larger with increasing voltage. The linear growth will be dominated by the maximum of the growth rate defining the fastest growing wave number k_{fg}. Given Eq. (57), one easily calculates

$$k_{fg} = \frac{4}{3\tilde{K}}\left(-\Gamma_\kappa + \sqrt{\Gamma_\kappa^2 - \frac{3}{16}\tilde{K}\tilde{\Sigma}}\right), \tag{58}$$

$$k_{\max} = \frac{2}{\tilde{K}}\left(-\Gamma_\kappa + \sqrt{\Gamma_\kappa^2 - \frac{1}{4}\tilde{K}\tilde{\Sigma}}\right), \tag{59}$$

for $\tilde{\Sigma}<0$.

The same information given by the dispersion relation can be expressed by the so-called neutral curve which is shown in Fig. 4(b). This curve, given by the solid line, separates the negative (below) from the positive (above) growth rates in the control parameter-wave number plane. If the voltage is below the section of the neutral curve with the voltage axis, the system is stable. Otherwise a certain band of wave numbers is unstable. The position of the fastest growing mode k_{fg} is given by the dashed line.

Since we have the dispersion relation in analytical form, in principle one has formulas for all relevant observables like the threshold voltage V_c. In terms of the system parameters, however, they are quite lengthy. The threshold voltage is given by the change of sign of the leading order contribution in $s(k_\perp)$. In the nonconductive case it has the simple form

$$V_c^2(G=0) = \frac{\Sigma_0 d(2+\kappa\lambda_m)^2}{\kappa(\kappa\epsilon_m\lambda_m^2+\epsilon d)}. \tag{60}$$

Since both ρ_m (and j_m in case of $G\neq 0$) are proportional to the voltage, as expected the critical voltage scales like $V_c \propto \sqrt{\Sigma_0}$. In the limit of small membrane conductance, one gets to leading order (using that L is macroscopic)

$$V_c^2 = V_c^2(G=0)\left(1+\frac{4GL}{\epsilon D\kappa^2}\right). \tag{61}$$

Thus membrane conductance increases the voltage value needed to cross the instability. In the limit of high salt, $\kappa \to \infty$, one regains the known result $V_c^2=\Sigma_0 d/\epsilon_m$. The typical wavelength of the membrane undulations above threshold (i.e., the one of the fastest growing mode) for parameters as in Fig. 4 is of order $\lambda=\frac{2\pi}{0.5\kappa}\simeq 0.25\ \mu\text{m}\simeq 12.5\lambda_D$, so several times the Debye length.

C. ICEO flows

We now discuss the form of the fluid flows which arise near the membrane when it is driven by ionic currents. Figure 5(c) shows the flow field for a high membrane conductivity and low salt, in the regime where the membrane is unstable due to the electrostatic correction to the surface tension and thus starts to undulate. This figure was generated by selecting the fastest growing wave number k_{fg}, defined in Sec. VI B, and using the respective maximum growth rate $s(k_{fg})$. Since this wave number has the fastest growth rate in the linear regime, it will dominate the initial behavior. The shape of the membrane undulation is represented as the black solid curves in all plots of Fig. 5. The resulting flow, shown in Fig. 5(c) is a superposition of two distinct flows: first, the typical flow associated to a membrane bending mode [41,42] as shown in Fig. 5(a). This contribution corresponds to the terms proportional to the growth rate s in Eqs. (44) and (45). Second, the flow associated with the remaining terms in Eqs. (44) and (45), proportional to α. This contribution yields the typical counter-rotating vortices of an ICEO flow [18], as shown in Fig. 5(b). Clearly, the superposition of these two flow contributions, as shown in Fig. 5(c), results in a parallel flow close to the membrane, in contrast to the usual bending mode flow given by Fig. 5(a).

Since the jump of the charge density $\rho_m>0$ for biological membranes (and $j_m\geq 0$ by definition), the induced flow occurs for this case in the same direction as in standard ICEO flows. Note that an inverse ICEO flow was obtained in [15], due to the opposite sign of ρ_m obtained with the simple but

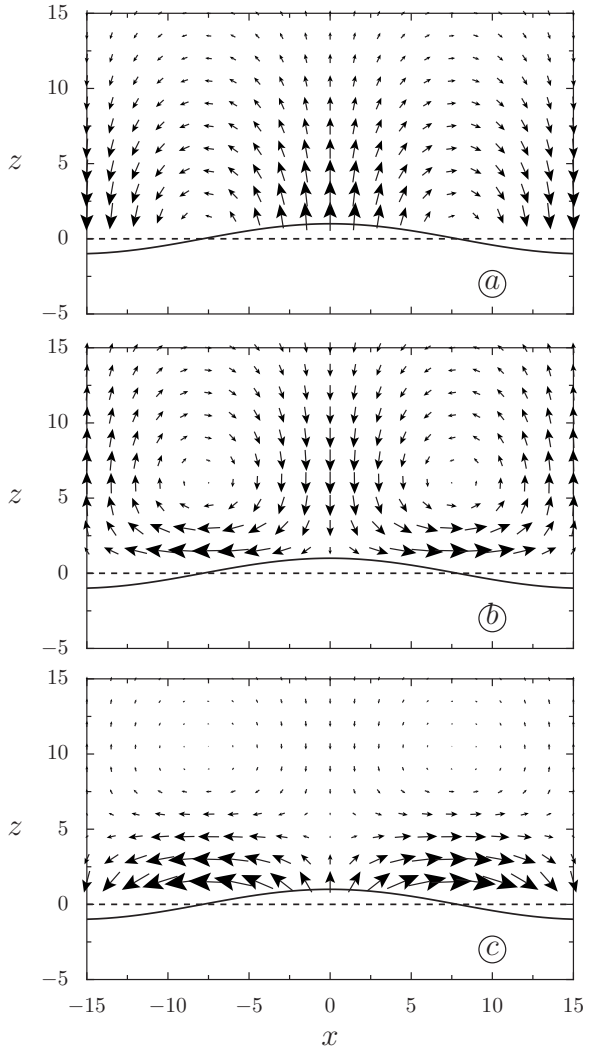

FIG. 5. Representation of the flows around the membrane beyond the instability threshold. The orientation of the electric field is toward negative values of z. Panel (a) shows the flow generated by the membrane bending instability [terms proportional to s in Eqs. (44) and (45)]. Panel (b) shows the ICEO flow [terms proportional to α in Eqs. (44) and (45)]. Finally, panel (c) shows the actual flow, which is the superposition of the former two and results in a strong flow near the membrane, oriented parallel to the surface. Both axes are scaled by the Debye length κ^{-1}. Parameters are as in previous figures except $V=3.165$ V, $\kappa=10^7$ m^{-1}, $G=10$ S m^{-2} and $L=10$ μm.

unrealistic BC Eq. (13). Also, the situation of ICEO flows is less general as suggested earlier: for most parameters (modest conductivities, not too low salt) the flow generated by membrane bending is usually dominating and hides the small ICEO contribution. This is due to the fact that the former is proportional to s which has contributions $\propto\rho_m^2$, while the ICEO flow is $\propto\rho_m j_m \ll \rho_m^2$. Thus, to see the situation given by Fig. 5, a high membrane conductance G is needed. Second, one needs low salt, since otherwise the membrane instability is shifted to very high voltages. Also, since for macroscopic electrode distances L (of order millimeter) and high conductance the voltage needed to induce the instability is very high, we have used a microscopic electrode distance $L=10$ μm. While it might still be possible to see these flows for higher salt and macroscopic electrode separations, such situations will be clearly far beyond the Debye-Hückel approximation used so far.

The ICEO flows near the membrane could also become relevant once the system has reached a steady state. Indeed in the case of lipid vesicles for instance, nonlinear effects associated with the conservation of the number of lipids on the vesicle [23] guarantee a saturation of the membrane fluctuations (for not too high voltages that might lead to vesicle rupture), as compared to the case of the planar membrane considered here. Since the membrane fluctuations are confined by nonlinear effects and become quasistationary in the long time limit, the system can reach a well defined nonequilibrium steady state. In this nonequilibrium steady state, fluid flows will persist due to ionic currents going through the membrane, after the transient flow associated with the membrane bending mode has disappeared.

D. Applications of the model to experiments

Recently, Lecuyer *et al.* [25] have investigated a pair of nearby membrane bilayers in an electric field by neutron reflectivity. The first bilayer was close to the bottom electrode and used to protect the second one from interacting with the wall. Since the bare values of the elastic moduli were known from x-ray off-specular experiments for a similar system [43] ($\Sigma_0 \simeq 0.5$ mN m^{-1} and $K_0 \simeq 40 k_B T$), the surface tension correction was extracted from the data under the assumption that the bending modulus is not affected by the field. The experiments were performed in an ac electric field at several frequencies. For the lowest frequency (10 Hz), the electrostatic correction to the surface tension was obtained to be $\Delta\Sigma \simeq -3$ mN m^{-1}.

In the experimentally probed regime of low salt (D_2O was used as the electrolyte), the electrostatic corrections to the elastic moduli depend rather sensitively on both the amount of salt and on the ionic conductance of the membrane, as discussed in Sec. VI A. Moreover, in the above experiment, the correction to the bending modulus was not measured. Thus we restrain ourselves to a comparison of orders of magnitude only. The distance between the electrodes was about $L=1$ mm, while the voltage was in the 1–5 V range. With the other parameters as used above, and assuming that the membrane is nonconductive, $G=0$, for $\kappa=2\cdot 10^7$ m^{-1} and $V=1$ V, our model yields $\Delta\Sigma \simeq -2\times$ mN m^{-1} and $\Delta K \simeq 190 k_B T$. The model thus successfully accounts for the order of magnitude of the electrostatic correction to the surface tension. However, it also shows that the bending modulus increases about five times. In order to obtain an experimental test of the model, it would be interesting to measure the correction to the surface tension and to the bending modulus simultaneously. We would also like suggest to carry out experiments in which the applied electric field or the ionic strength would be varied. Another interesting possibility would be to study membranes of different conductivities or thicknesses in an applied electric field.

A second field of application of the model are active membranes, which are (artificial) lipid vesicles containing

ionic pumps such as bacteriorhodopsin [7–9]. In these experiments, no external electric field is applied. Instead the pumps are activated by light to transport protons across the membrane. In Ref. [9], a lowering of the membrane tension produced by the activity of the pumps has been reported, which could be due to an accumulation of charges near the membrane, as discussed here. The specificity of that experiment is that this charge accumulation would result from the activity of the pumps rather than from an applied electric field. However, it is difficult to make a precise comparison between the experiments and the present theory, because only the correction to the surface tension is accurately measured and many aspects of the transport of ions are unknown. Nevertheless, if we assume that the passive state of that experiment corresponds to a nonconductive membrane ($G=0$) and the active state to a membrane with $G=10$ S m^{-2}, and if we use a typical transmembrane potential of the order of 50 mV, we get the same order of magnitude for the observed tension lowering, 3×10^{-7} N m^{-1}, if we account for the rather high amount of salt with $\kappa\simeq5\times10^{8}$ m^{-1}. We also find that there is no measurable difference for the bending modulus between the active and passive state, as observed experimentally. The model predicts that a current density of $j_m\simeq1$ Am^{-2} arises when the pumps are active, which corresponds to an overall current of 1pA on a vesicle of size 1 μm. To better compare to the model, again it would be desirable to have experiments in varying conditions (ionic strength and conductance of the membrane, for instance). Another interesting possibility would be to measure the membrane current and the transmembrane potential in the course of the experiment, for instance using patch-clamp techniques.

VII. CONCLUSIONS AND PERSPECTIVE

This paper offers a route to describe capacitive effects near a conductive lipid membrane while keeping the simplicity of the zero thickness approximation on which most of the literature on lipid membranes is based. These capacitive effects are the main player in the corrections to the elastic moduli of membranes driven by an electric field or by internal pumps or ionic channels. The present theory goes beyond available descriptions by including nonequilibrium effects which arise due to ionic membrane currents. These ionic currents have a similar form as the ICEO flows studied in the context of microfluidics and can modify the fluid flows around the membrane from usual bending dominated flow.

Our approach is sufficiently simple to be the starting point for further generalizations, which could include various nonlinear effects: nonlinear elastic terms associated with the membrane or the cytoskeleton in case of a biological membrane, nonlinear current-voltage response of the channels. Also density fluctuations of the ion channels and the experimentally simpler case of an ac electric field should be investigated. Further theoretical work is also needed to extend the model to higher voltage where the Debye-Hückel approximation breaks down. In fact, this approximation only holds when the potential satisfies everywhere the condition $\frac{e\phi}{4k_BT}\ll1$ [16]. For the experiments on supported membranes discussed above, one finds that the charge accumulation on the membrane is too large for this approximation to hold, since one has $\frac{e\phi}{4k_BT}\simeq2$. It would thus be relevant to solve the nonlinear Poisson-Nernst-Planck equations and otherwise proceed similarly as proposed in this work, in order to describe the behavior of membranes surrounded by high charge densities. Furthermore, it would be interesting to investigate a model suitable for small system sizes, since much of the results of this paper are based on the assumption that the system size L is much larger than all other length scales in the problem, as well as for more realistic boundary conditions at the electrodes.

We would like to thank Thierry Charitat and Pierre Sens for fruitful discussions and Luis Dinis for a careful reading of the manuscript. F.Z. acknowledges financial support from the German Science Foundation (DFG), M.Z.B. support from the U.S. National Science Foundation under Contract No. DMS-0707641 and D.L. from the Indo-French Center for the Promotion of Advanced Research under Grant No. 3502 and ANR for funding.

APPENDIX A: ELECTROSTATICS TO FIRST ORDER IN $h(\mathbf{r}_\perp)$

From the expansion of the potential given in Eq. (32), and using the equation of ion conservation and Poisson's equation, one obtains the following equations to first order in membrane height:

$$(\partial_z^2-k_\perp^2)\phi_1(\mathbf{k}_\perp,z)+\frac{2}{\epsilon}\rho_1(\mathbf{k}_\perp,z)=0, \tag{A1}$$

$$(\partial_z^2-k_\perp^2)\left[\rho_1(\mathbf{k}_\perp,z)+\frac{\epsilon}{2}\kappa^2\phi_1(\mathbf{k}_\perp,z)\right]=0, \tag{A2}$$

and for the particle currents at the membrane one has the condition

$$D\partial_z\left(\rho_1+\frac{\epsilon}{2}\kappa^2\phi_1\right)_{|z=h}=G\left(\frac{2}{\epsilon\kappa^2}[\rho_1]_{z=0}+[\phi_1]_{z=0}\right). \tag{A3}$$

Since we assumed $L\gg\lambda_D$, we can use $\phi_1(\mathbf{k}_\perp,\pm\infty)=\rho_1(\mathbf{k}_\perp,\pm\infty)=0$ far from the membrane, and Eqs. (A2) and (A3) and the BCs at infinity are satisfied by choosing $\rho_1=-\frac{\epsilon}{2}\kappa^2\phi_1$ (and $n_1^+=-n_1^-$ implying $\rho_1=en_1^+$). It follows that to first order in the height, one has a zero flux condition at the membrane. Accordingly, the zeroth order solution enters in the equations for the first-order solution ϕ_1 only via the boundary conditions.

It thus remains to solve the Poisson equation (A1),

$$(\partial_z^2-k_\perp^2-\kappa^2)\phi_1=0. \tag{A4}$$

Introducing $l^2=k_\perp^2+\kappa^2$ one easily gets $\phi_1=A^{\mp}e^{\mp lz}$ for $z>0$ and $z<0$ respectively. To determine the constants $A^{\pm}$, one expands

$$\partial_z\phi_{|z=h(\mathbf{r}_\perp)} = \partial_z\phi_{0|z=0} + \partial_z^2\phi_{0|z=0}\cdot h(\mathbf{r}_\perp) + \partial_z\phi_{1|z=0} + O(h^2), \tag{A5}$$

to prescribe the BC at the membrane in first order. Using this expansion in the Robin-type BC we get Eqs. (34).

APPENDIX B: CALCULATION OF THE STRESSES AT THE MEMBRANE

The total normal stress at the membrane is

$$\tau_{zz,1} = \left[-P + 2\eta\partial_z v_z + \frac{\epsilon}{2}(\partial_z\phi)^2 - \frac{\epsilon_m}{2}(\partial_z\phi^m)^2\right]_{|z=h} \tag{B1}$$

to linear order in h. Note that we have included here the electrostatic contribution stemming from the field inside the membrane (with potential ϕ^m). This contribution is particularly significant in the high-salt limit, where effects due to the Debye layers become negligible. This inside contribution enters with opposite sign than the outside contribution because of the difference of orientation of the normal (see Appendix C and Ref. [19]).

The outer electrostatic contribution reads

$$\epsilon[(\partial_z\phi_0)(\partial_z\phi_1)]_{|z=0} + h\partial_z\left[-P_0 + \frac{\epsilon}{2}(\partial_z\phi_0)^2\right]_{|z=0},$$

where the second contribution vanishes since the term in the bracket is a constant (the stress is balanced, see above). The electrostatic contribution from inside the membrane can be expressed analogously, and the normal-normal stress difference at the membrane reads

$$[\tau_{zz,1}]_{z=0} = -[p]_{z=0} + 2\eta[\partial_z v_z]_{z=0} + \epsilon[(\partial_z\phi_0)(\partial_z\phi_1)]_{z=0} - \epsilon_m[(\partial_z\phi_0^m)(\partial_z\phi_1^m)]_{z=\pm d/2}. \tag{B2}$$

By means of Eq. (44) one easily verifies $[\partial_z v_z]_{z=0}=0$ due to the symmetry given above. For the pressure difference, Eq. (46) implies $[p]_{z=0}=2p(0^+)$ and after reexpressing l by $k_\perp$ and expanding in powers of $k_\perp$, one obtains

$$[p]_{z=0} = h(\mathbf{k}_\perp)\left[8\left(\frac{\rho_m j_m}{\epsilon D\kappa^2} + \frac{\rho_m^2}{\epsilon\kappa}\right) + 4\eta s k_\perp + 4\left(-\frac{\rho_m^2}{\epsilon\kappa^3} - \frac{4\rho_m j_m}{\epsilon D\kappa^4}\right)k_\perp^2 + 16\frac{\rho_m j_m}{\epsilon D\kappa^5}k_\perp^3 + 3\frac{\rho_m^2}{\epsilon\kappa^5}k_\perp^4\right]. \tag{B3}$$

The electrostatic contribution from the electrolyte reads

$$\epsilon[(\partial_z\phi_0)(\partial_z\phi_1)]_{z=0} = h(\mathbf{k}_\perp)8\left(\frac{\rho_m j_m}{\epsilon D\kappa^2} + \frac{\rho_m^2}{\epsilon\kappa}\right), \tag{B4}$$

which exactly cancels the $k_\perp$-independent contribution of $[p]_0$.

The calculation of the electrostatic contribution from inside the membrane is slightly more involved. This contribution reads

$$[\tau_{zz,1}^m]_{z=0} = \epsilon_m[(\partial_z\phi_0^m)(\partial_z\phi_1^m)]_{z=\pm d/2}. \tag{B5}$$

Since the internal field at zeroth order is constant inside the membrane due to the symmetry of the problem, this expression simplifies into

$$[\tau_{zz,1}^m]_{z=0} = -2\epsilon_m E_0^m(\partial_z\phi_1^m)_{|z=+d/2}. \tag{B6}$$

The first-order field in the membrane is given by (use the symmetry or cf. Ref. [15] for details)

$$\phi_1^m(k_\perp,z) = \phi_1^m(k_\perp,d/2)\frac{e^{k_\perp d/2}}{e^{k_\perp d}+1}(e^{k_\perp z}+e^{-k_\perp z}), \tag{B7}$$

which leads us to

$$[\tau_{zz,1}^m]_{z=0} = -2\epsilon_m E_0^m\phi_1^m\left(k_\perp,\frac{d}{2}\right)k_\perp\frac{e^{k_\perp d}-1}{e^{k_\perp d}+1}. \tag{B8}$$

To obtain an expression for $\phi_1^m(k_\perp,\frac{d}{2})$, to linear order in h, one can write [15]

$$\phi_1^m\left(k_\perp,\frac{d}{2}\right) = \phi_1\left(k_\perp,\frac{d}{2}\right) - h(\partial_z\phi_0^m - \partial_z\phi_0)_{|z=d/2}. \tag{B9}$$

For the outside potential at the membrane we can approximately use $\phi_1(k_\perp,z)=-\frac{2}{\epsilon}\rho_m\frac{h(k_\perp)}{l}$ here (since the exponential decay like e^{-lz} starts at the membrane). After expansion in $k_\perp$ (and assuming $L\gg d$) we get

$$\phi_1^m\left(k_\perp,\frac{d}{2}\right) = h(k_\perp)\left[E_0^m + \frac{\rho_m}{\epsilon\kappa^3}k_\perp^2\right]. \tag{B10}$$

Using Eq. (B8), for the stress difference, $[\tau_{zz,1}^m]_{z=0}$, up to order $k_\perp^4$ this yields

$$\epsilon_m[(\partial_z\phi_0^m)(\partial_z\phi_1^m)]_{z=\pm d/2} = -h(\mathbf{k}_\perp)\epsilon_m(E_0^m)^2\left[dk_\perp^2 + \left(-\frac{d^3}{12} + \frac{\rho_m}{E_0^m}\frac{d}{\epsilon\kappa^3}\right)k_\perp^4\right]. \tag{B11}$$

APPENDIX C: ELECTROSTATIC CONTRIBUTION TO THE SURFACE TENSION FROM THE STRESS TENSOR

In this appendix, we give an alternative approach for the derivation of the membrane tension, which avoids solving for the fluid flow around the membrane. Here the tension is expressed as an integral over the lateral pressure profile deviation or, equivalently, over the excess lateral stress [44].

Let us call S a closed surface englobing the membrane with the normal vector field $\mathbf{n}$. We choose $\mathbf{x}$ to represent the direction of the lateral stress. The force acting on the surface S in the $\mathbf{x}$ direction can be calculated from the stress tensor defined in Eq. (28) as

$$F_x = \int_S \mathbf{x}\cdot\tau\cdot\mathbf{n}dS. \tag{C1}$$

Since τ is divergence free, the surface S can be deformed into an arbitrary other surface englobing S, for convenience to a cube of size L. It is easy to see that the integral in Eq. (C1) is nonzero only on the faces of the cube with the normal along $\pm\mathbf{x}$. With $dS=Ldz$ and $\Delta\Sigma=F_x/L$ on the face where $\mathbf{n}=+\mathbf{x}$, we arrive at [19]

$$\Delta\Sigma = \int_{-L/2}^{L/2} \tau_{xx}(z)dz. \tag{C2}$$

Equation (28) implies $\tau_{xx}(z) = -P_0(z) - \frac{\epsilon}{2}(\partial_z \phi_0)^2$, where $\phi_0(z)$ is the potential and $P_0(z)$ the pressure profile in the base state. The resulting tension $\Delta\Sigma$ is identical to Eqs. (41)–(43) of Ref. [15], where it was expressed as a sum of two terms, Σ_0 and Σ_1. A cancellation of the dependence on L occurred in the sum of these two terms, as it should be. The present derivation fully justifies this point since the choice of the deformed surface was arbitrary by construction. Using Eqs. (18), (29), and (C2), we obtain

$$\Delta\Sigma_\kappa = -4\frac{\rho_m^2}{\epsilon\kappa^3} - 16\frac{\rho_m j_m}{\epsilon\kappa^4 D}, \tag{C3}$$

which is exactly the result for the contribution of the Debye layers to the tension using the hydrodynamic approach, Eq. (50). A similar calculation gives contribution to the tension from inside the membrane, which reads

$$\Delta\Sigma_m = -\epsilon_m d(E_m^0)^2. \tag{C4}$$

Note that the same method could be used to calculate the change of spontaneous curvature induced by an electric potential in the asymmetric case [19].

[1] U. Seifert, Adv. Phys. **46**, 13 (1997).
[2] D. Andelman, *Handbook of Biological Physics*, edited by R. Lipowsky and E. Sackmann (Elsevier, Amsterdam, 1995), Vol. 1A.
[3] E. Neumann, A. E. Sowers, and C. A. Jordan, *Electroporation and Electrofusion in Cell Biology* (Plenum Press, New York, 1989).
[4] B. Hille, *Ion Channels of Excitable Membranes* (Sinauer Press, Sunderland, 2001).
[5] J. Prost and R. Bruinsma, Europhys. Lett. **33**, 321 (1996).
[6] S. Ramaswamy, J. Toner, and J. Prost, Phys. Rev. Lett. **84**, 3494 (2000).
[7] J. B. Manneville, P. Bassereau, D. Lévy, and J. Prost, Phys. Rev. Lett. **82**, 4356 (1999).
[8] J. B. Manneville, P. Bassereau, S. Ramaswamy, and J. Prost, Phys. Rev. E **64**, 021908 (2001).
[9] M. D. El Alaoui Faris, D. Lacoste, J. Pécréaux, J. F. Joanny, J. Prost, and P. Bassereau, Phys. Rev. Lett. **102**, 038102 (2009).
[10] N. Gov, Phys. Rev. Lett. **93**, 268104 (2004).
[11] S. Sankararaman, G. I. Menon, and P. B. Sunil Kumar, Phys. Rev. E **66**, 031914 (2002).
[12] H.-Y. Chen, Phys. Rev. Lett. **92**, 168101 (2004).
[13] M. A. Lomholt, Phys. Rev. E **73**, 061913 (2006); **73**, 061914 (2006).
[14] D. Lacoste, M. Cosentino Lagomarsino, and J.-F. Joanny, Europhys. Lett. **77**, 18006 (2007).
[15] D. Lacoste, G. I. Menon, M. Z. Bazant, and J. F. Joanny, Eur. Phys. J. E **28**, 243 (2009).
[16] R. J. Hunter, *Foundations of Colloid Science* (Oxford University Press, Oxford, 2001).
[17] A. Ajdari, Phys. Rev. E **61**, R45 (2000); A. González, A. Ramos, N. G. Green, A. Castellanos, and H. Morgan, *ibid.* **61**, 4019 (2000).
[18] M. Z. Bazant and T. M. Squires, Phys. Rev. Lett. **92**, 066101 (2004).
[19] T. Ambjörnsson, M. A. Lomholt, and P. L. Hansen, Phys. Rev. E **75**, 051916 (2007).
[20] V. Kumaran, Phys. Rev. E **64**, 011911 (2001); R. M. Thaokar and V. Kumaran, *ibid.* **66**, 051913 (2002); V. Kumaran, Phys. Rev. Lett. **85**, 4996 (2000).
[21] M. Leonetti, E. Dubois-Violette, and F. Homblé, Proc. Natl. Acad. Sci. U.S.A. **101**, 10243 (2004).
[22] P.-C. Zhang, A. M. Keleshian, and F. Sachs, Nature (London) **413**, 428 (2001).
[23] P. Sens and H. Isambert, Phys. Rev. Lett. **88**, 128102 (2002).
[24] D. Constantin, C. Ollinger, M. Vogel, and T. Salditt, Eur. Phys. J. E **18**, 273 (2005).
[25] S. Lecuyer, G. Fragneto, and T. Charitat, Eur. Phys. J. E **21**, 153 (2006).
[26] V. A. Murtsovkin, Colloid J. **58**, 341 (1996) [Kolloidn. Zh. **58**, 358 (1996)].
[27] T. M. Squires and M. Z. Bazant, J. Fluid Mech. **509**, 217 (2004).
[28] M. Staykova, R. Lipowsky, and R. Dimova, Soft Matter **4**, 2168 (2008).
[29] P. M. Vlahovska, R. S. Graci, S. Aranda-Espinoza, and R. Dimova, Biophys. J. **96**, 4789 (2009).
[30] P. Peterlin, S. Svetina, and B. Zeks, J. Phys.: Condens. Matter **19**, 136220 (2007).
[31] R. Dimova *et al.*, Soft Matter **3**, 817 (2007).
[32] M. Z. Bazant, K. T. Chu, and B. J. Bayly, SIAM J. Appl. Math. **65**, 1463 (2005); K. T. Chu and M. Z. Bazant, *ibid.* **65**, 1485 (2005).
[33] F. Divet, G. Danker, and C. Misbah, Phys. Rev. E **72**, 041901 (2005).
[34] M. Z. Bazant, M. S. Kilic, B. D. Storey, and A. Ajdari, Adv. Colloid Interface Sci. **152**, 48 (2009).
[35] M. Z. Bazant, K. Thornton, and A. Ajdari, Phys. Rev. E **70**, 021506 (2004).
[36] P. M. Biesheuvel, M. van Soestbergen, and M. Z. Bazant, Electrochim. Acta **54**, 4857 (2009).
[37] E. M. Itskovich, A. A. Kornyshev, and M. A. Vorotyntsev, Phys. Status Solidi A **39**, 229 (1977).
[38] A. Bonnefont, F. Argoul, and M. Bazant, J. Electroanal. Chem. **500**, 52 (2001).
[39] S. Chatkaew and M. Léonetti, Eur. Phys. J. E **17**, 203 (2005); M. Léonetti and E. Dubois-Violette, Phys. Rev. Lett. **81**, 1977 (1998).
[40] T. Bickel, Phys. Rev. E **75**, 041403 (2007).
[41] F. Brochard and J. F. Lennon, J. Phys. (Paris) **36**, 1035 (1975).
[42] A. J. Levine and F. C. MacKintosh, Phys. Rev. E **66**, 061606 (2002).
[43] J. Daillant *et al.*, Proc. Natl. Acad. Sci. U.S.A. **102**, 11639 (2005).
[44] J. S. Rowlinson and B. Widom, *Molecular Theory of Capillarity* (Oxford University Press, Oxford, 1982).